ionocast: A Real-Time HF/VHF Propagation Prediction Model for Amateur Radio Operators

Toprak Kilic, TA1BUT

`flayzeraynx@gmail.com`

April 2026

Abstract

ionocast provides real-time HF/VHF band-condition verdicts and 3–12 hour forward projections for amateur radio operators. The model runs entirely in the browser with no server-side state; the operator's QTH never leaves the device. It combines an ITU-R P.533–grounded SNR link budget with real-time data from NOAA SWPC (solar indices, D-RAP absorption, OVATION auroral power), the kc2g ionosonde network (observed MUF and foF2), GIRO digisondes (foF2, foEs, hmF2), and WSPR spot observations from `wspr.live`. A 70/30 ensemble blend with an N0NBH-style SFI heuristic anchors predictions to community-calibrated expectations, while a local validation harness corrects systematic bias via per-group, per-horizon offsets derived from retrospective WSPR scoring. Key contributions include an *asymmetric MUF consensus* that trusts observations over climatology when the ionosphere is declining, a *power-summed noise model* that correctly handles man-made noise dominance on the low bands, and *per-hop minimum MUF* via great-circle ray geometry. All computation is deterministic, repeatable, and inspectable—no machine-learning black boxes.

Contents

1 Introduction

Amateur radio operators planning an operating session need to answer a deceptively simple question: *which bands will be open, and for how long?* The answer depends on the instantaneous state of the ionosphere, the Sun, the geomagnetic field, and the operator's own station—antenna, power, mode, and local noise environment.

Existing tools serve fragments of this problem:

- **VOACAP** [1] provides rigorous P.533-based predictions but operates as a batch tool requiring manual circuit specification; it is not real-time.
- **N0NBH Solar Conditions** provides a widely trusted heuristic band-condition table keyed to SFI and Kp, but without path geometry or operator context.
- **kc2g MUF map** renders observed MUF contours in near real time, but offers no forward projection and no SNR context.
- **HamQSL / DX Toolbox** use threshold-based rules on solar indices, lacking physics grounding.

ionocast occupies the intersection: real-time, physics-grounded, operator-configurable, and privacy-preserving. The operator's QTH (stored in `localStorage` only) parameterises five reference propagation paths; the SNR budget runs per band, per path, per time-step. Forward projections at +3, +6, +9, and +12 hours use solar-zenith analogy, storm depression, seasonal correction, and sporadic-E persistence.

This paper documents the complete model as implemented, with every numeric constant, so that the amateur radio community can audit, reproduce, and improve it.

2 Data Sources

Table 1 lists all upstream data feeds. Sources marked "Direct CORS" are fetched by the browser with no server proxy; sources marked "Proxied" pass through a Cloudflare Worker endpoint that resolves the operator's Maidenhead grid to a station identifier server-side.

Table 1: Upstream data sources and refresh cadences.

Source	**Data**	**Refresh**	**Protocol**
NOAA SWPC	Kp, Ap, F10.7, X-ray class, 3-day forecast, 27-day outlook, D-RAP HAF, OVATION aurora HP, solar-wind Bz/speed/density, solar regions	1–10 min	Direct CORS JSON/text
prop.kc2g.com	Per-station MUF(3000F2), foF2, TEC	∼15 min	Direct CORS JSON
GIRO (lgdc.uml.edu)	Nearest digisonde foF2, foEs, hmF2	∼10 min	Proxied via `/api/giro`
GFZ Potsdam	Hp30 nowcast	30 min	Proxied via `/api/hp30`
WDC Kyoto	Dst / Sym-H	1 h	Proxied via `/api/kyoto`
SILSO	Daily sunspot number	Daily	Proxied via `/api/silso`
UWyo	Radiosonde soundings (ΔN for tropo)	12 h	Proxied via `/api/tropo`
wspr.live	WSPR spot counts and SNR by band	10 min	Direct CORS (ClickHouse)
NASA DONKI	CME and HSS analyses	∼hours	Direct CORS JSON

2.1 Privacy Model

The operator's QTH is stored exclusively in `localStorage` and never transmitted to any ionocast server. WSPR queries use only the two-character Maidenhead field (an ∼18°×20° rectangle), providing geographic context without meaningful localisation. Proxied endpoints (`/api/giro`, etc.) resolve the QTH to the nearest station code server-side; the response contains only station data, not the query coordinates.

3 SNR Budget Model

The core of ionocast is a complete link budget that computes the SNR margin M (in dB) for each amateur band on each reference path:

$$M = P_{\text{tx}} + G_{\text{ant}} - L_{\text{fs}} - L_{\text{abs}} - L_{\text{absD}} - L_{\text{aur}} - L_{\text{MUF}} - L_{\text{iono}} - L_{\text{low}} - L_{\text{hop}} - L_{\text{Es}} - N - S_{\text{req}} \quad (1)$$

where every term is defined in the following subsections. A positive M means the signal exceeds the minimum required SNR for the chosen mode; the magnitude indicates robustness.

3.1 Free-Space Loss (Friis / ITU-R P.525)

$$L_{\text{fs}} = 32.44 + 20\log_{10}(d_{\text{km}}) + 20\log_{10}(f_{\text{MHz}}) \quad (2)$$

The distance d_{km} is the great-circle path length, clamped to a minimum of 50 km to avoid numerical singularity on extremely short paths.

3.2 MUF Approach and Over-MUF Loss (ITU-R P.533 §3.2.2)

Let $r = f/\text{MUF}$. The proximity loss is:

$$L_{\text{MUF}} = \begin{cases} 0 & r \le 0.70 \\ 10\left(\dfrac{r - 0.70}{0.30}\right)^2 & 0.70 < r \le 1.00 \\ 10 + 36\sqrt{r-1} & r > 1.00 \end{cases} \quad (3)$$

Below 70% of MUF the ionosphere provides comfortable refraction with negligible loss. Between 70–100% the loss rises quadratically. Above MUF (over-MUF operation, e.g. via Es or scatter), the loss escalates rapidly.

3.3 D-Region Absorption—Flare-Enhanced (SWPC D-RAP)

SWPC's D-RAP product provides a Highest Affected Frequency (HAF) in MHz. The flare-enhanced absorption is:

$$L_{\text{abs}} = \begin{cases} 0 & \text{HAF}/f < 0.3 \\ 3\left(\dfrac{\text{HAF}}{f}\right)^{1.5} & \text{otherwise} \end{cases} \quad (4)$$

3.4 D-Region Absorption—Quiet-Day Diurnal (ITU-R P.533 §4)

$$L_{\text{absD}} = A_{\text{base}}(f) \cdot (\cos\chi)^{1.3} \quad (5)$$

where χ is the solar zenith angle at the path midpoint. At night ($\cos\chi < 0.05$), $L_{\text{absD}} = 0$. The base absorption values follow K9LA quiet-day estimates (Table 2).

Table 2: Quiet-day D-region base absorption A_{base} by band.

Band	A_{base} (dB)
160 m	28
80 m	18
60 m	10
40 m	6
30 m	2
20 m	0.5
15 m+	0

3.5 Auroral Absorption (CGM-Gated)

Auroral absorption activates only when the corrected geomagnetic (CGM) latitude of the path midpoint satisfies $|\phi_{\text{CGM}}| \geq 60°$:

$$L_{\text{aur}} = \min\left(30,\ D \cdot \frac{30}{f_{\text{MHz}}}\right) \tag{6}$$

where

$$D = \max\left(5(K_p - 4),\ \frac{\text{HP}_{\text{GW}} - 50}{5}\right) \tag{7}$$

when either $K_p \geq 5$ or the OVATION hemispheric power HP ≥ 50 GW.

The CGM latitude is computed via a tilted-dipole approximation:

$$\phi_{\text{CGM}} = \arcsin\bigl(\sin\phi \sin\phi_P + \cos\phi \cos\phi_P \cos(\lambda - \lambda_P)\bigr) \tag{8}$$

with the IGRF 2020 north magnetic pole at $\phi_P = 80.7°\text{N}$, $\lambda_P = 72.7°\text{W}$.

3.6 Multi-Hop Ground Reflection Loss

Each ground reflection costs 5 dB:

$$L_{\text{hop}} = 5\,(N_{\text{hops}} - 1) \quad \text{dB}, \qquad N_{\text{hops}} = \lceil d_{\text{km}}/4000 \rceil \tag{9}$$

3.7 Sporadic-E Screening Loss

When a strong Es layer is present ($f_{\text{oEs}} \geq 5$ MHz) and the operating frequency is below twice the Es critical frequency ($f < 2\,f_{\text{oEs}}$), the layer partially screens the F2 reflection:

$$L_{\text{Es}} = 5\,\text{dB} \tag{10}$$

3.8 Low-Band Extra Loss

A step-function accounts for additional empirical losses on the lower HF bands (ground-wave coupling, higher-angle refraction, congestion):

Band	L_{low} (dB)
160 m	8
80 m	5
60 m	3
40 m	2
30 m+	0

3.9 Lumped Ionospheric Loss

$$L_{\text{iono}} = 15\,\text{dB} \tag{11}$$

This lumps three P.533 terms that are not individually modelled: spatial focusing/defocusing $L_z \approx 3\,\text{dB}$, above-median variability plus polarisation coupling $Y_p \approx 9\,\text{dB}$, and residual terms $\approx$3 dB. It does *not* include D-region absorption (handled by L_{absD} and L_{abs}) or ground reflection (handled by L_{hop}).

3.10 Noise Model (ITU-R P.372)

The received noise power is computed as a *power sum* of atmospheric and man-made components, ensuring the total never drops below the galactic/man-made floor:

$$N = 10\log_{10}\left(10^{N_{\text{atmo}}/10} + 10^{N_{\text{mm}}/10}\right) \tag{12}$$

where:

$$N_{\text{atmo}} = N_{\text{base}}(f) + \Delta N_{\text{diurnal}}(f, \cos\chi) \tag{13}$$

$$N_{\text{mm}} = N_{\text{base}}(f) + F_a \tag{14}$$

The diurnal swing is:

$$\Delta N_{\text{diurnal}} = -A \cdot \text{clamp}(\cos\chi,\ -1,\ 1) \tag{15}$$

with $A = 10\,\text{dB}$ for $f \leq 10\,\text{MHz}$ and $A = 3\,\text{dB}$ above. The man-made noise factor F_a depends on environment: rural 0 dB, suburban +15 dB, urban +25 dB.

Table 3 gives the baseline noise power at 2.5 kHz reference bandwidth.

Table 3: Baseline noise N_{base} from ITU-R P.372 at 2.5 kHz bandwidth.

Band	N_{base} (dBm)
160 m	-110
80 m	-115
60 m	-118
40 m	-122
30 m	-125
20 m	-128
17 m	-131
15 m	-132
12 m	-133
10 m	-134

3.11 Required SNR by Mode

Mode	S_{req} (dB)
SSB	+10
CW	+3
FT8	-21
FT4	-13
WSPR	-25

3.12 Default Operator Settings

The default station profile assumes a typical amateur installation: $P_{\text{tx}} = 50\,\text{dBm}$ (100 W), $G_{\text{ant}} = +5\,\text{dBi}$ (installed dipole with ground reflection), mode = SSB, noise environment = suburban.

3.13 Worked Example: 20 m, 3000 km, Quiet Day

Figure 1 illustrates the complete budget for a 14.1 MHz path of 3000 km on a quiet day.

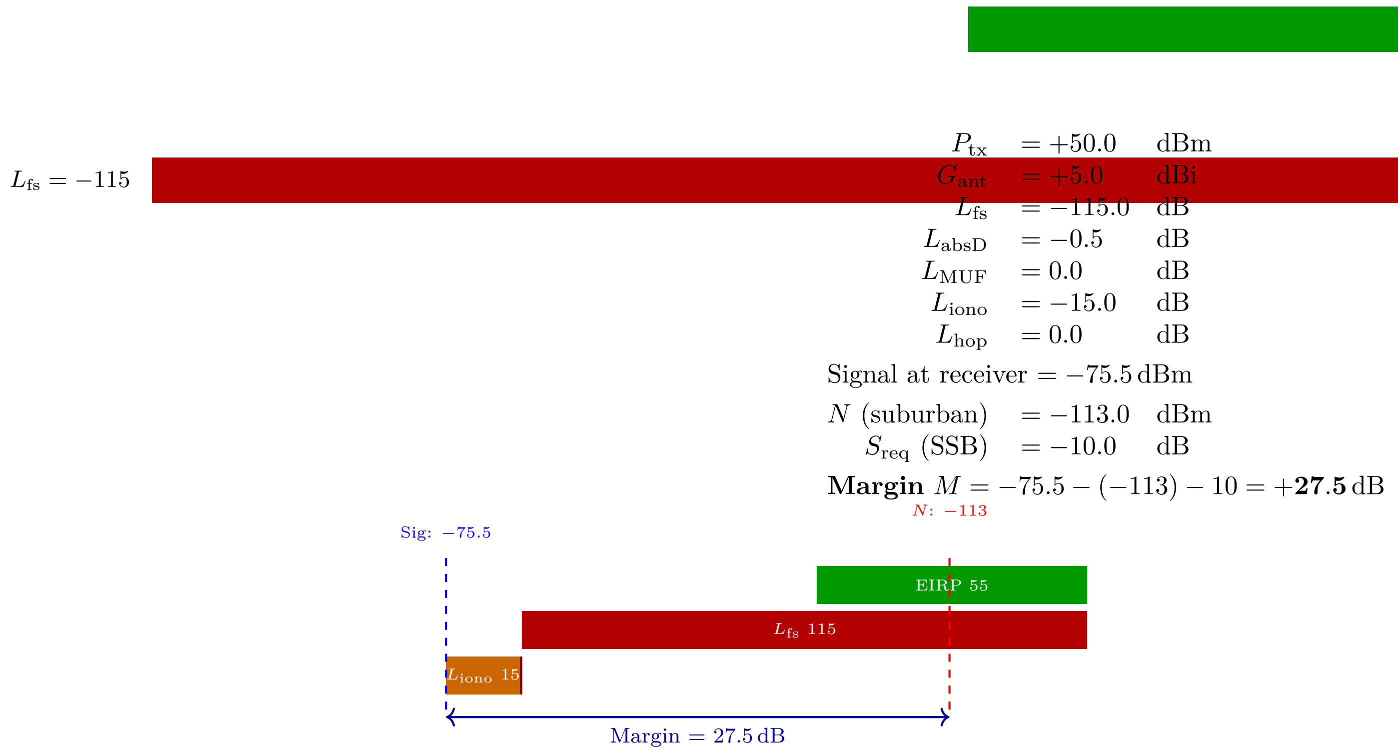

$P_{\text{tx}} = +50.0$ dBm
$G_{\text{ant}} = +5.0$ dBi
$L_{\text{fs}} = -115.0$ dB
$L_{\text{absD}} = -0.5$ dB
$L_{\text{MUF}} = 0.0$ dB
$L_{\text{iono}} = -15.0$ dB
$L_{\text{hop}} = 0.0$ dB
Signal at receiver $= -75.5\,\text{dBm}$
N (suburban) $= -113.0$ dBm
S_{req} (SSB) $= -10.0$ dB
Margin $M = -75.5 - (-113) - 10 = +\mathbf{27.5}\,\text{dB}$

Figure 1: SNR budget waterfall for 20 m (14.1 MHz), 3000 km, quiet day, suburban noise, SSB. The 27.5 dB margin corresponds to an "Excellent" verdict.

4 MUF Estimation

The Maximum Usable Frequency is the single most important input to the link budget. ionocast derives it from three sources in a consensus blend.

4.1 kc2g Observed MUF

The kc2g network publishes MUF(3000F2) from each ionosonde. For each of five reference paths (midpoints near New York, São Paulo, Johannesburg, Tokyo, Sydney), ionocast selects the nearest ionosonde. A *freshness gate* discards observations older than 30 min.

4.2 foF2 Climatology (Simplified P.1239)

When observed data are stale or unavailable, ionocast falls back to a simplified climatological model:

$$f_{\text{oF2}} = \max(2,\ (3.5 + 0.04(F_{10.7\text{A}} - 70)) + 4.0(1 - 0.003|\phi|) \cdot \max(0, \cos\chi)) \qquad (16)$$

with $\mathrm{MUF}(3000) \approx 3.0 \times f_{\mathrm{oF2}}$.

4.3 Asymmetric Consensus Blend

The consensus algorithm treats upward and downward divergence differently, reflecting the physical asymmetry that a declining ionosphere (afternoon/evening) is far more common than spurious low station readings:

1. Compute divergence: $\delta = |\ln(\mathrm{MUF}_{\mathrm{kc2g}}/\mathrm{MUF}_{\mathrm{climo}})|$
2. If $\delta \leq \ln 1.5$: use the geometric mean $\sqrt{\mathrm{MUF}_{\mathrm{kc2g}} \cdot \mathrm{MUF}_{\mathrm{climo}}}$
3. If kc2g $<$ climatology (declining ionosphere): **trust kc2g**
4. If kc2g $>$ climatology (possible station anomaly): **fall to climatology**

4.4 Per-Hop Minimum MUF (P.533 §3.1)

For paths requiring $N \geq 2$ hops, each reflection point at fraction $(2k-1)/(2N)$ along the great circle may see a different solar illumination. The path MUF is the *minimum* across all hops:

$$\mathrm{MUF}_{\mathrm{path}} = \min_{k=1}^{N} \mathrm{MUF}_{\mathrm{mid}} \cdot \frac{S(\cos\chi_k,\, F)}{S(\cos\chi_{\mathrm{mid}},\, F)} \tag{17}$$

where $S(c, F) = \max(F,\, \sqrt{\max(0.05,\, c)})$ is the zenith-shape function and F is the night floor.

4.5 Night Floor (CCIR/IRI)

The night floor scales with solar activity and latitude:

$$F = \mathrm{clamp}\left(0.25 + 0.0025(F_{10.7\mathrm{A}} - 70) - 0.10 \min\left(1,\, \frac{|\phi|}{60}\right),\ 0.20,\ 0.60\right) \tag{18}$$

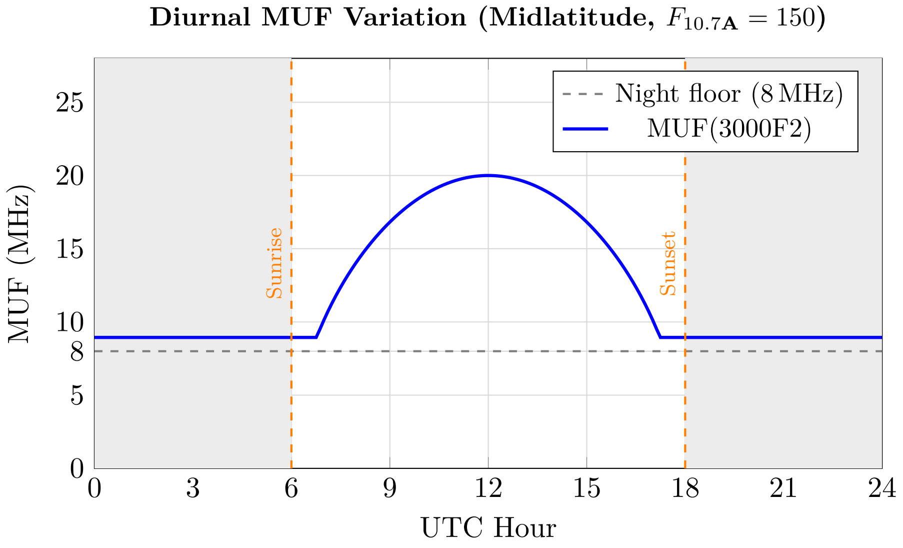

Figure 2: Diurnal MUF variation showing the $\sqrt{\cos\chi}$ shape scaled to a peak of 20 MHz with night floor at 8 MHz (shaded regions = night).

5 Forward Projection (3–12 h)

The forward projection engine extends the current nowcast into the future by modelling the dominant drivers of ionospheric change.

5.1 MUF Projection via Solar Zenith Analogy

$$\mathrm{MUF}_{\mathrm{future}} = \mathrm{MUF}_{\mathrm{now}} \cdot \frac{S(\cos\chi_{\mathrm{future}},\, F)}{S(\cos\chi_{\mathrm{now}},\, F)} \cdot R_{\mathrm{seasonal}} \cdot F_{\mathrm{storm}} \tag{19}$$

5.2 Seasonal Ratio

$$R_{\mathrm{seasonal}} = \frac{s(t_{\mathrm{future}},\, \phi)}{s(t_{\mathrm{now}},\, \phi)} \tag{20}$$

where

$$s(t, \phi) = 1 + (0.15\cos\theta + 0.08\cos(2\theta + \pi)) \cdot w(\phi) \tag{21}$$

with $\theta = (m - 1 - h \cdot 6) \cdot 2\pi/12$, h being the hemisphere flag ($+1$ north, -1 south), and $w(\phi) = \min(1, |\phi|/50)$. The first term captures the annual winter-peak/summer-trough at midlatitudes; the second captures the semi-annual equinox peaks (March, September) evident in F2-layer statistics.

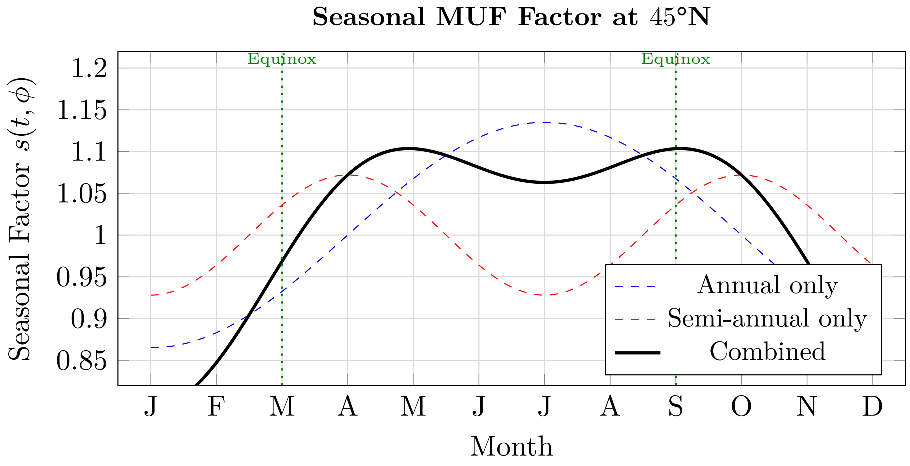

Figure 3: Seasonal MUF factor at 45°N showing annual (winter peak) and semi-annual (equinox peaks) components.

5.3 Storm Depression

When $K_p > 4$, the MUF is depressed:

$$F_{\mathrm{storm}} = \max(0.5,\ 1 - p\,(K_p - 4)) \tag{22}$$

where

$$p = 0.05 + 0.10 \cdot \mathrm{clamp}\left(\frac{|\phi_{\mathrm{CGM}}| - 40}{30},\ 0,\ 1\right) \tag{23}$$

At midlatitudes ($|\phi_{\mathrm{CGM}}| = 40°$), the damping is 5% per K_p unit above 4. In the auroral zone ($|\phi_{\mathrm{CGM}}| = 70°$), it rises to $\sim$15% per unit.

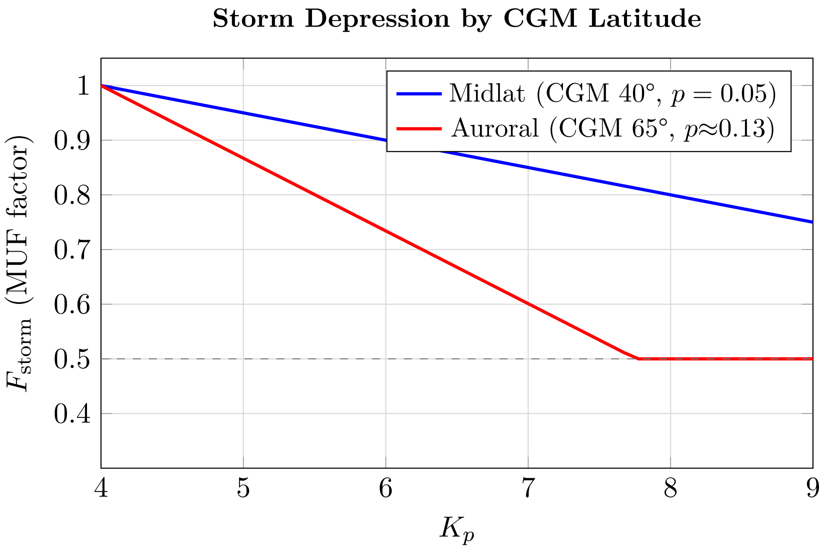

Figure 4: Storm MUF depression factor vs. K_p for midlatitude and auroral-zone paths. The floor is clamped at 0.5 (50% depression).

5.4 Sporadic-E Persistence

The projected critical frequency of the sporadic-E layer decays exponentially:

$$f_{\text{oEs}}(t+\Delta) = \max\Big(B,\ f_{\text{oEs}}(t)\cdot 2^{-\Delta/\tau}\Big) \tag{24}$$

with half-life $\tau = 1.5\,\text{h}$ at night, $3.0\,\text{h}$ during the day. The background $B = 2\,\text{MHz}$ when $\cos\chi > 0.2$, otherwise 0.

5.5 Gray-Line Bonus

On 160–80 m, when the path midpoint lies near the terminator ($|\cos\chi| < 0.1$), a bonus of up to +5 dB is applied to reflect the reduced D-region absorption at the gray line.

6 Ensemble Blend and Self-Calibration

6.1 Blended Margin

The final margin is a weighted average of the physics-based model and a community-calibrated heuristic:

$$M_{\text{blend}} = 0.7\,(M_{\text{physics}} + B_{g,\Delta h}) + 0.3\,M_{\text{heuristic}} \tag{25}$$

6.2 N0NBH-Style Heuristic

The heuristic encodes rules similar to N0NBH's SFI/Kp-based band condition table, returning a tier that maps to a dB equivalent:

Heuristic Tier	$M_{\text{heuristic}}$ (dB)
Excellent	+20
Good	+10
Fair	0
Poor	-10
Closed	-18

6.3 Bias Correction from Validation Harness

The self-calibration harness (Section 6) accumulates retrospective scoring against WSPR observations. The bias correction per band group g and forecast horizon Δh is:

$$B_{g,\Delta h} = 11 \cdot \overline{(r_{\text{actual}} - r_{\text{predicted}})} \quad \text{dB} \tag{26}$$

where r denotes the tier index (Excellent=4, . . . , Closed=0) and the factor 11 converts tier-units to dB using the constant tier width. The correction activates only when $n \geq 10$ scored samples exist; below threshold, $B = 0$.

6.4 Tier Probabilities

Given the blended margin M and spread $\sigma = 8\,\text{dB}$ (ITU-R P.533 typical range 6–10 dB), the probability of achieving at least tier T is:

$$P(\text{tier} \geq T) = 1 - \Phi\left(\frac{\theta_T - M}{\sigma}\right) \tag{27}$$

where Φ is the standard normal CDF and θ_T is the tier threshold (Table 4).

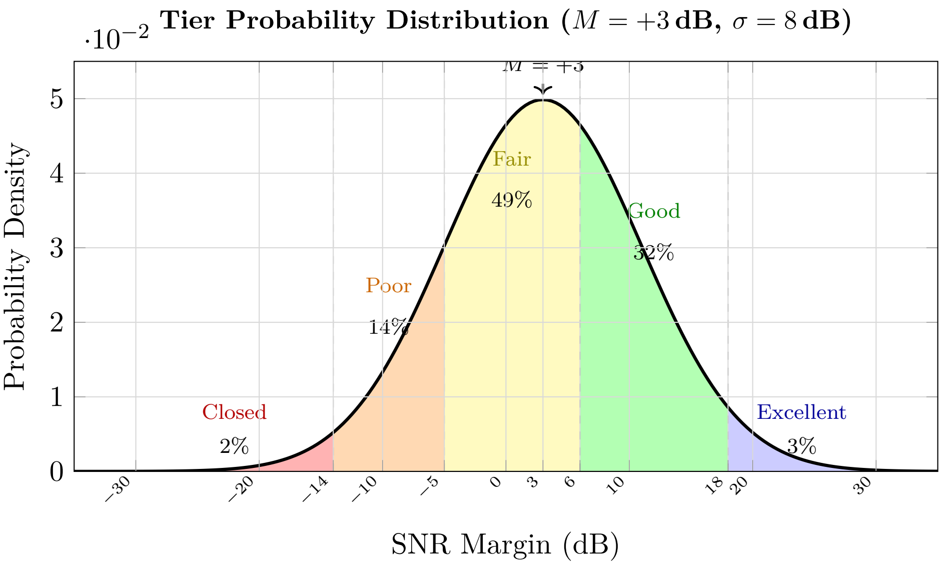

Figure 5: Tier probability distribution for a blended margin of +3 dB with $\sigma = 8$ dB. The most likely tier is Fair (49%), with a 35% chance of Good or better.

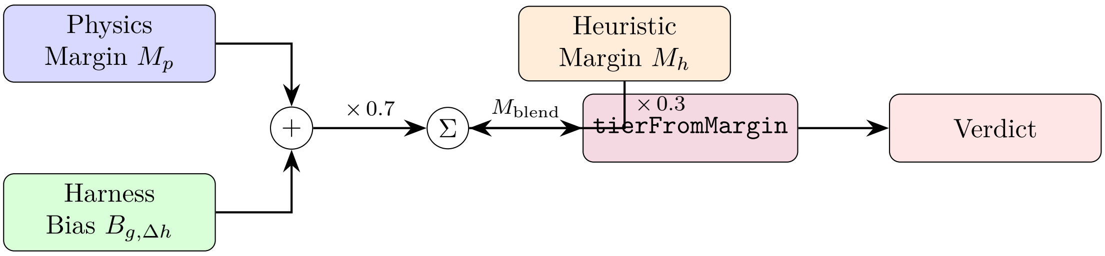

Figure 6: Ensemble blend flow diagram. The physics margin (with harness bias correction) receives 70% weight; the N0NBH-style heuristic receives 30%.

7 Tier Mapping

The continuous margin is discretised into five operator-facing tiers (Table 4).

Table 4: Tier thresholds.

Tier	Margin Threshold (dB)	**Meaning**
Excellent	$\geq +18$	Signals well above noise; reliable copy
Good	$\geq +6$	Comfortable contacts expected
Fair	≥ -5	Marginal; digital modes work, SSB intermittent
Poor	≥ -14	Weak/absent signals; only FT8/WSPR viable
Closed	< -14	Band effectively closed

7.1 WSPR Spot-Reality Override

When WSPR spot counts for a band exceed the activity threshold but the model predicts Poor or Closed, the verdict is overridden to Fair. This “reality check” prevents the model from contradicting observable evidence—if real signals are propagating, the band is not closed.

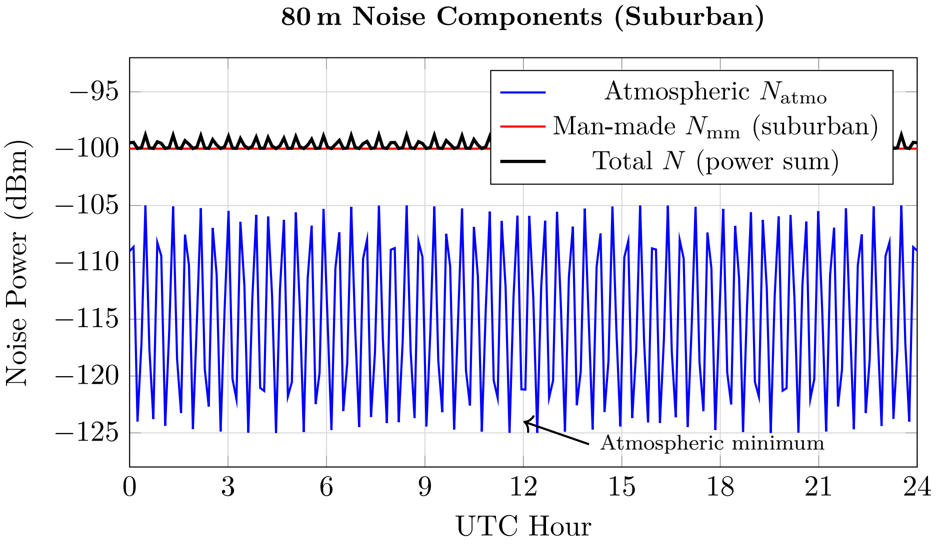

Figure 7: Noise power components on 80 m in a suburban environment. The man-made noise (-100 dBm) dominates at all hours; the atmospheric diurnal swing barely affects the total. This power-sum model prevents the phantom 7 dB margin that a linear (dB-domain) sum would produce at midday.

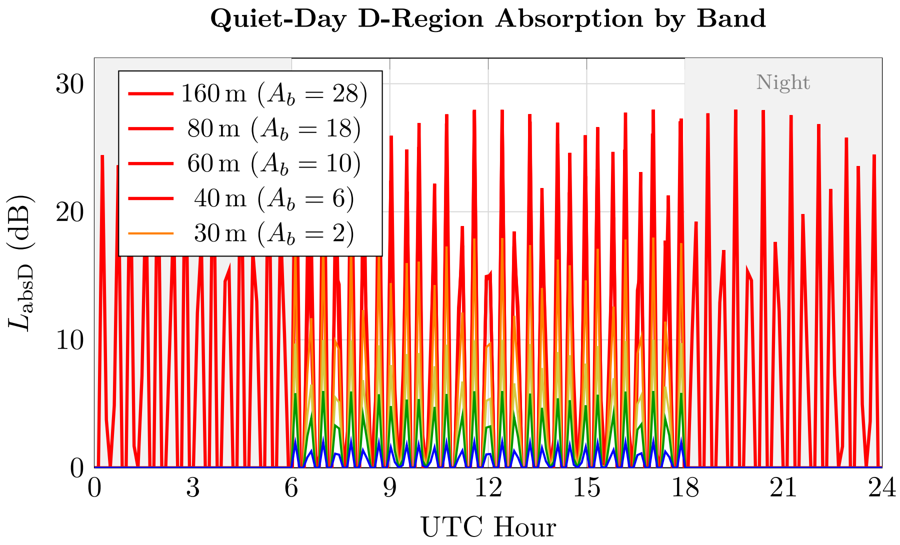

Figure 8: Quiet-day D-region absorption by band. 160 m reaches 28 dB at local noon; 30 m and above are essentially unaffected. Night absorption is zero.

8 Known Limitations and Future Work

1. **No antenna takeoff-angle pattern.** The antenna is modelled as a single gain scalar. Real antennas have elevation-dependent patterns; a $\lambda/4$-high dipole has a low-angle null that can bury 10–20 dB of long-haul signal. This is the single largest per-user accuracy improvement pending.
2. **No NVIS for short paths ($<$ 500 km).** The model defaults to multi-hop DX geometry. Near-vertical-incidence skywave on 80/40 m uses vertical-incidence MUF ($\approx$ foF2) rather than MUF(3000).
3. **Dst and IMF Bz fetched but not used in the model.** These indices are displayed in the UI but do not yet feed into the storm depression or nowcast logic.
4. **Validation harness needs 2–4 weeks for meaningful skill scores.** Until sufficient WSPR-scored samples accumulate, the bias correction defaults to zero and sigma to 8 dB.
5. **Condition-dependent σ not yet implemented.** The spread is fixed at 8 dB. In reality, variance increases near MUF ($f/\mathrm{MUF} > 0.85$), during storms ($K_p \geq 5$), and on cross-terminator paths.
6. **No short-path vs. long-path evaluation.** Only the short great-circle path is evaluated. Long-path openings (classic at dawn/dusk on 20 m) are missed.

9 References

References

[1] ITU-R Recommendation P.533-14, *Method for the Prediction of the Performance of HF Circuits*, International Telecommunication Union, Geneva, 2019.

[2] ITU-R Recommendation P.372-14, *Radio Noise*, International Telecommunication Union, Geneva, 2019.

[3] ITU-R Recommendation P.1239-3, *ITU-R Reference Ionospheric Characteristics*, International Telecommunication Union, Geneva, 2015.

[4] ITU-R Recommendation P.525, *Calculation of Free-Space Attenuation*, International Telecommunication Union, Geneva.

[5] ITU-R Recommendation P.534, *Method for Calculating Sporadic-E Field Strength*, International Telecommunication Union, Geneva.

[6] ITU-R Recommendation P.842, *Computation of Reliability and Compatibility of HF Radio Systems*, International Telecommunication Union, Geneva.

[7] ARRL, *The ARRL Antenna Book* and *The ARRL Handbook for Radio Communications*, 2023 editions, American Radio Relay League, Newington, CT.

[8] C. Luetzelschwab (K9LA), "Quiet-day D-region absorption tables," personal communication and online articles, `https://www.k9la.us/`.

[9] J. H. Taylor (K1JT), "WSJT-X: Digital Modes for Weak Signal Communications," `https://wsjt.sourceforge.io/wsjtx.html`.

[10] T. J. Fuller-Rowell, M. V. Codrescu, R. G. Roble, and A. D. Richmond, "How does the thermosphere and ionosphere react to a geomagnetic storm?" in *Magnetic Storms*, Geophysical Monograph 98, pp. 203–225, American Geophysical Union, 1994.

[11] M. Mendillo, "Storms in the ionosphere: Patterns and processes for total electron content," *Reviews of Geophysics*, vol. 44, RG4001, 2006. DOI: 10.1029/2005RG000193.

[12] G. W. Prölss, "Ionospheric F-region storms," in *Handbook of Atmospheric Electrodynamics*, vol. 2, pp. 195–248, CRC Press, 1995.

A Default Settings

Table 5: Default operator settings.

Parameter	**Default Value**	**Notes**
Transmit power P_{tx}	50 dBm (100 W)	Typical HF transceiver
Antenna gain G_{ant}	+5 dBi	Installed dipole w/ ground reflection
Mode	SSB	$S_{\text{req}} = +10\,\text{dB}$
Noise environment	Suburban	$F_a = +15\,\text{dB}$
Reference bandwidth	2.5 kHz	SSB passband
Spread σ	8 dB	ITU-R P.533 typical-day
Ensemble weights	0.7 / 0.3	Physics / heuristic
Tier width	11 dB	For bias ↔ dB conversion
kc2g freshness gate	30 min	Stale data discarded
Hop distance	4000 km	Assumes $h_F = 300\,\text{km}$

B Noise Floor Table

Table 6: NOISE_FLOOR_DBM table with ITU-R P.372 cross-reference. Values at 2.5 kHz reference bandwidth. Man-made noise offset F_a is added to N_{base} for each environment.

Band	f (MHz)	N_{base} (dBm)	Rural (dBm)	Suburban (dBm)	Urban (dBm)
160 m	1.8	-110	-110	-95	-85
80 m	3.5	-115	-115	-100	-90
60 m	5.3	-118	-118	-103	-93
40 m	7.0	-122	-122	-107	-97
30 m	10.1	-125	-125	-110	-100
20 m	14.1	-128	-128	-113	-103
17 m	18.1	-131	-131	-116	-106
15 m	21.1	-132	-132	-117	-107
12 m	24.9	-133	-133	-118	-108
10 m	28.1	-134	-134	-119	-109

The P.372 external noise figure F_a for galactic noise is incorporated into N_{base}. The suburban and urban columns show the man-made floor $N_{\text{mm}} = N_{\text{base}} + F_a$ that dominates the power sum in most residential environments.